Domain Decomposition with Patched Subgrids

K.H. TAN[1] and M.J.A. BORSBOOM [2]

1 ABSTRACT

This paper describes a domain decomposition method for advection-diffusion problems on a two-dimensional domain that has been subdivided into a number of non-overlapping subdomains, each covered by its own structured grid. The discretization of the problem's PDE over the entire domain is based on local finite difference discretizations on each subgrid, together with several so-called coupling equations that are needed to couple the discrete solution at subdomain interfaces. The choice of coupling equations depends on the discrete problem at hand and should result in a fast converging overall iterative procedure, at the same time maintaining sufficient accuracy of the solution across the interfaces. We show how both requirements can be fulfilled within the approach of optimized parameterized interface conditions when the grid at the interfaces is non-smooth, thereby extending our previous work on regularly patched Cartesian grids.

2 INTRODUCTION

One of the main issues in domain decomposition is the specification of suitable interface conditions at the artificially introduced internal boundaries of subdomains.

[1] Delft Hydraulics, Dept S&O, P.O. Box 152, 8300 AD Emmeloord, the Netherlands, Kian.Tan@wldelft.nl

[2] Delft Hydraulics, Dept S&O, P.O. Box 152, 8300 AD Emmeloord, the Netherlands, Mart.Borsboom@wldelft.nl

Domain Decomposition Methods in Sciences and Engineering, edited by R. Glowinski *et al.*

Obviously, the order of accuracy of the discretization inside the subdomains should be retained over the interfaces. Also physical requirements like mass conservation should be fulfilled. At the same time however, these internal boundary conditions should be designed for fast convergence of the overall iterative solution procedure that pieces together the global solution from the solutions of the different subproblems.

In this paper we propose a method for constructing such proper interface conditions in grid patching for the coupling of the solution of non-overlapping subdomains, each having its own grid. They can be regarded as discretizations of so-called coupling equations, involving suitably chosen combinations of several derivatives which are expressed in either a global coordinate system or a local computational coordinate system. The performance of the resulting domain decomposition algorithm is illustrated for the two-dimensional model problem

$$\frac{\partial c}{\partial t} + v_1 \frac{\partial c}{\partial x} + v_2 \frac{\partial c}{\partial y} = D\left(\frac{\partial^2 c}{\partial x^2} + \frac{\partial^2 c}{\partial y^2}\right) \text{ on } \Omega \ , D > 0 \ , \quad c = g \text{ on } \Gamma_i \ . \tag{1}$$

Here, Γ_i denotes those parts of the boundary where Dirichlet inflow conditions are imposed. On the remaining part of the boundary $\delta\Omega \backslash \Gamma_i$ we specify outflow conditions, based on one-sided discretizations of the advection part of (1).

3 THE MODEL PROBLEM ON NON-OVERLAPPING SUBDOMAINS

Consider problem (1) on a number of naturally ordered parallelograms Ω_k,

$$\Omega = \bigcup_{k=1}^{K} \Omega_k \qquad \Omega_k \cap \Omega_{k+1} = \Gamma_{kk+1} = \Gamma_{k+1k} \qquad k = 1, \ldots, K-1 \ .$$

An example of a strip decomposition which we consider is given in Figure 1.

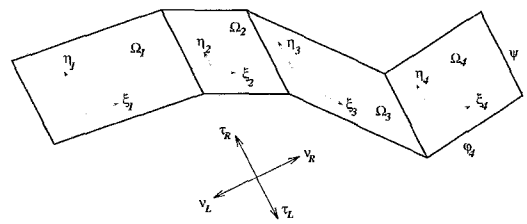

Figure 1 Example of a strip decomposition.

Prior to the discretization, (1) is transformed on each subdomain to a local coordinate system. We consider on each subdomain k the linear transformation $\xi_k = \xi_k(x, y)$, $\eta_k = \eta_k(x, y)$, that transforms Ω_k to a rectangle in computational space:

$$J_k = \begin{pmatrix} \frac{\partial x}{\partial \xi_k} & \frac{\partial y}{\partial \xi_k} \\ \frac{\partial x}{\partial \eta_k} & \frac{\partial y}{\partial \eta_k} \end{pmatrix} = \begin{pmatrix} h_{\xi_k} & 0 \\ 0 & h_{\eta_k} \end{pmatrix} \begin{pmatrix} \cos\phi_k & \sin\phi_k \\ -\sin\psi & \cos\psi \end{pmatrix} . \tag{2}$$

with $-\frac{\pi}{2} < \phi_k - \psi < \frac{\pi}{2}$. The resulting transformed equations are then discretized in the local, i.e. per subdomain, computational coordinate system, for which uniform Cartesian grids are employed. Without loss of generality we may assume that each local Cartesian grid has mesh size 1, since the actual mesh size in physical space can be included in the transformation via scalars h_{ξ_k} and h_{η_k}.

To keep our discussion of coupling clear, we consider only grid lines in ξ_k-direction that connect at the interfaces, i.e. $h_{\eta_k} = h_\eta$, $\forall k$. To facilitate the specification of the discrete equations holding at the subdomain boundaries, the local grids extend beyond both the physical and internal boundaries, these boundaries lying *in between* the outer two layers of grid points. See Figure 2, where the bold lines indicate the boundaries of subdomains. The □- and •-points indicate the locations where respectively boundary conditions and coupling conditions are discretized (cf. Section 4).

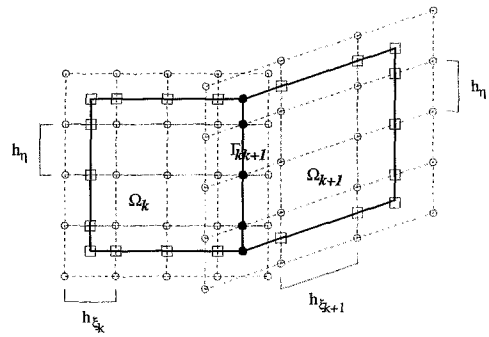

Figure 2 Two subdomains and two local grids.

For later purposes it is convenient to define transformations with respect to the normal and tangential direction at interfaces as well. Let ν_{kk+1} and ν_{k+1k} denote the unit outward normal (at the interface) to Ω_k and Ω_{k+1}. Tangential vectors τ_{kk+1} and τ_{k+1k} are defined as the vectors that are obtained by rotating ν_{kk+1} and ν_{k+1k} counterclockwise. For our decomposition, we have that $\forall k$, $\nu_{kk+1} = \nu_R$, $\tau_{kk+1} = \tau_R$, $\nu_{k+1k} = \nu_L$, and $\tau_{k+1k} = \tau_L$. The local coordinate transformations $\xi_k(\nu_R, \tau_R), \eta_k(\nu_R, \tau_R)$ and $\xi_k(\nu_L, \tau_L), \eta_k(\nu_L, \tau_L)$ are still defined by transformation matrices of the form (2), but with the rotation angles ϕ_k and ψ replaced by $\hat{\phi}_k = \phi_k - \psi$, $\hat{\psi} = 0$ and $\bar{\phi}_k = -\pi + \phi_k - \psi$, $\bar{\psi} = \pi$, respectively.

The transformed equations that are discretized per subdomain k are:

$$\frac{\partial c_k}{\partial t} + v_1^k \frac{\partial c_k}{\partial \xi_k} + v_2^k \frac{\partial c_k}{\partial \eta_k} = D_{\xi\xi}^k \frac{\partial^2 c_k}{\partial {\xi_k}^2} + D_{\eta\eta}^k \frac{\partial^2 c_k}{\partial {\eta_k}^2} + D_{\xi\eta}^k \frac{\partial^2 c_k}{\partial \xi_k \eta_k} \text{ on } \Omega_k \,, \tag{3}$$

with transformed velocities and diffusion coefficients v_1^k, v_2^k, $D_{\xi\xi}^k$, $D_{\eta\eta}^k$, and $D_{\xi\eta}^k$. Its discretization is given in Section 4.

3.1 Coupling equations

The key point of this paper is the construction of equations that provide an accurate and fast coupling of the individual solutions c_k at the interfaces Γ_{kk+1}. From a

continuous point of view, it is sufficient to impose (see e.g. [QL88])

$$\frac{\partial c_k}{\partial \nu_{kk+1}} = \frac{\partial c_{k+1}}{\partial \nu_{kk+1}} \text{ on } \Gamma_{kk+1} \qquad k = 1, \ldots, K-1\,, \qquad [\curvearrowleft] \quad (4a)$$

$$c_{k+1} = c_k \text{ on } \Gamma_{k+1k} \qquad k = 1, \ldots, K-1\,. \qquad [\curvearrowright] \quad (4b)$$

The multi-domain formulation (3)–(4b) is then equivalent with the original problem (1), since $c|_{\Omega_k} = c_k$. Note that for each interface $\Gamma_{kk+1} = \Gamma_{k+1k}$ two conditions are formulated. For comparison with the discrete conditions that follow, we have listed them as conditions for either subdomain k ($[\curvearrowleft]$) or subdomain $k+1$ ($[\curvearrowright]$). For obvious reasons these conditions are called coupling conditions, or interface conditions. As indicated in e.g. [Tan92] it is allowed to use more general conditions

$$\Phi_{kk+1}(c_k) = \Phi_{kk+1}(c_{k+1}) \text{ on } \Gamma_{kk+1} \qquad k = 1, \ldots, K-1\,, \qquad [\curvearrowleft] \quad (5a)$$

$$\Phi_{k+1k}(c_{k+1}) = \Phi_{k+1k}(c_k) \text{ on } \Gamma_{k+1k} \qquad k = 1, \ldots, K-1\,, \qquad [\curvearrowright] \quad (5b)$$

as long as they imply conditions (4a) and (4b). This seems to be an academic matter only, would it not be that these conditions have a significant influence on the rate of convergence of the solution procedure for the global discrete problem. This has motivated the authors to develop coupling equations involving more general operators:

$$\begin{aligned} \Phi_{ij} \equiv \quad & \zeta_{ij}\left(I + h_\eta \beta_{ij}\frac{\partial}{\partial \tau_{ij}} + (h_\eta)^2 \delta_{ij}\frac{\partial^2}{\partial {\tau_{ij}}^2}\right) + \\ & h_{\xi_j}\alpha_{ij}\frac{\partial}{\partial \nu_{ij}}\left(I + h_\eta \gamma_{ij}\frac{\partial}{\partial \tau_{ij}} + (h_\eta)^2 \epsilon_{ij}\frac{\partial^2}{\partial {\tau_{ij}}^2}\right)\,, \end{aligned} \qquad (6)$$

where i, j are either $k, k+1$ or $k+1, k$, depending on the direction in which the coupling operator is used. Scalars h_{ξ_j} and h_η are the mesh size coefficients in transformations (2).

In equation (6), ζ_{ij}, α_{ij}, β_{ij}, γ_{ij}, δ_{ij}, and ϵ_{ij} are coupling *functions* from $\Gamma_{ij} \to \mathbb{R}$, not coefficients. It is clear that these functions have to satisfy certain conditions to guarantee equivalence of the multi-domain problem with the single-domain problem. The imposed conditions should still imply (4a)–(4b), which is already obtained as soon as Φ_{kk+1} and Φ_{k+1k} are distinctive enough.

In the remaining of this paper we assume the coupling functions to be optimized for convergence speed following the strategy of [Tan95]. This optimization of coupling functions turns out to provide equivalence automatically.

4 The model problem on virtually overlapping local grids

Having specified the entire continuous multi-domain problem we now consider its discretization on local grids of size $(n_{x_k} + 2) \times (n_y + 2)$. We refer to Figure 2 for a schematic diagram of the location of grid points in the two-subdomain case. The discrete multi-domain problem consists of:

- a standard 9-point discretization based on central differences of the transformed equations (3) at the $n_{\xi_k} \times n_\eta$ 'inner' grid points of each subdomain;

- a discretization of the boundary conditions at the □-points with 3×2- or 2×3-point (at the corners 2×2-point) computational molecules;
- discrete equivalents of coupling equations, applied at the •-points;
- backward Euler time discretization.

4.1 discrete coupling equations

Obviously, the spatial discretization of (1) in the interior grid points is second-order accurate. Our aim is to formulate discrete analogues of coupling equations that do not affect this accuracy. Hereto we employ a similar two-step discretization as used for (1). We first transform the continuous coupling equations (5a)–(5b) to the local coordinate systems and then discretize the result with 2×3 stencils.

Note that because of the choice of the stencil, we are unable to discretize all terms of the transformed coupling equations. So we (have to) neglect all terms containing second derivatives in ξ_k and ξ_{k+1}, which includes certain mixed derivatives.

As a consequence, discretized coupling equations contain both transformation and discretization errors. In order to quantify them, let $\bar{c}_k$ and $\bar{c}_{k+1}$ be the exact solutions of the discrete coupling equations, satisfying:

$$(\Phi_{kk+1} + \tilde{T}_{\Phi_{kk+1}} + \tilde{D}_{\Phi_{kk+1}})(\bar{c}_k) = (\Phi_{kk+1} + \breve{T}_{\Phi_{kk+1}} + \breve{D}_{\Phi_{kk+1}})(\bar{c}_{k+1}) \ , \quad [\curvearrowleft] \tag{7a}$$

$$(\Phi_{k+1k} + \breve{T}_{\Phi_{k+1k}} + \breve{D}_{\Phi_{kk+1}})(\bar{c}_{k+1}) = (\Phi_{k+1k} + \tilde{T}_{\Phi_{k+1k}} + \tilde{D}_{\Phi_{k+1k}})(\bar{c}_k) \ . \quad [\curvearrowright] \tag{7b}$$

The T-terms and D-terms represent transformation and discretization errors.

We will first address the size of the transformation errors.

Proposition 4.1 *Let Φ_{kk+1} be of the form (6) ($\nu_{kk+1} = \nu_R$, $\tau_{kk+1} = \tau_R$). Consider the coordinate systems $(\xi_k(\nu_R, \tau_R), \eta_k(\nu_R, \tau_R))$ and $(\xi_{k+1}(\nu_R, \tau_R), \eta_{k+1}(\nu_R, \tau_R))$ which specify the angles $\hat{\phi}_k$ and $\hat{\phi}_{k+1}$ between de interface and the ξ_k and ξ_{k+1} axis. Then*

$$\tilde{T}_{\Phi_{kk+1}}(c_k) = \ -h_{\xi_{k+1}}(h_\eta)^2 \alpha_{kk+1} \epsilon_{kk+1} \tan\hat{\phi}_k \cdot \frac{\partial^3 c_k}{\partial \tau_R^3} \ , \tag{8}$$

$$\breve{T}_{\Phi_{kk+1}}(c_{k+1}) = \ -h_{\xi_{k+1}}(h_\eta)^2 \alpha_{kk+1} \epsilon_{kk+1} \tan\hat{\phi}_{k+1} \cdot \frac{\partial^3 c_{k+1}}{\partial \tau_R^3} \ . \tag{9}$$

A similar proposition holds for Φ_{k+1k}.

This proposition shows that transformation errors increase with increasing skewness of the ξ-coordinate direction with respect to ν_R, as expected. However, for reasonable grid connections, i.e. when $\hat{\phi}_k - \hat{\phi}_{k+1} \approx 0$, transformation errors almost entirely cancel out, since they are made in *both* left- and right-hand side of the coupling equations.

Even when the transformation errors do not cancel, they can still be acceptable. From (8) and (9) it follows that these errors are of third or second order in the grid spacing, depending on whether the leading term of the coupling operators is zeroth or first order. The former applies when the coupling condition has an important Dirichlet component, while the latter applies when the coupling consists of Neumann plus higher derivatives. Of course, this second or third order transformation error is only acceptable when coefficients like $\epsilon_{kk+1}(\tan\hat{\phi}_{k+1} - \tan\hat{\phi}_k) < \mathcal{O}(1)$ (cf. (8)–(9)).

As for the discretization errors we remark that the D-terms in (7a)–(7b) are $\mathcal{O}((h_{\xi_k})^2) + \mathcal{O}((h_\eta)^2)$. The same important remark as for the transformation errors can be made here. Discretization errors in coupling equations tend to cancel out when grid connections are not too irregular, i.e. when $h_{\xi_k} - h_{\xi_{k+1}} \approx 0$. Note that it is the difference between the angle of subgrids at both sides of the interface that is important in the transformation errors, while it is change in the mesh size in ξ-direction that is important in the discretization errors.

Summarizing, the discretized interface conditions provide a second-order accurate coupling between the solutions per subdomain, which error tends to cancel out for small differences in subgrid angles and mesh sizes. This brings us to the conclusion that for the type of decomposition and discretization considered in this paper, the coupling at interfaces is an entirely transparent process. The discrete solution behaves as if no interfaces would have been present. This is also illustrated by taking $\phi_k = \phi$, $h_{\xi_k} = h_\xi$, $\forall k$, in which case overlapping grid points actually coincide. Then our approach automatically reduces to our coupling technique for regularly patched grids ([TB93]), which can be regarded as nothing else but a preconditioning technique for the discrete system of equations, without altering its solution.

We remark that the cancellation of discretization and transformation errors in interface conditions is entirely due to the special extension of the subgrids over the interface with the interface itself in between. Note also that our discrete coupling, by the simple fact of discretizing (5a)–(5b) automatically includes some form of interpolation.

5 Numerical experiments

The entire set of equations to be solved each time step can be represented by a block tridiagonal system $Bc = f$. Its principal submatrices B_{kk} represent the discretization of (3) in the interior of each of the subdomains, together with the discretized boundary conditions and the left-hand sides of the subsequent discrete coupling equations. Off-diagonal blocks only contain the right-hand sides of the discrete coupling equations. This system $Bc = f$ is solved by GCR [EES83], applied to the right-preconditioned system $BM^{-1}Mc = f$. The preconditioner M is taken as $M = \text{blockdiag}(B_{11}, \ldots, B_{KK})$. ILU(2)-preconditioned BiCGSTAB(4) ([SF93]) is used for solving up to sufficient precision the subsystems $B_{kk}u_k = r_k$ that occur during the GCR process.

The first example deals with a simple advection problem on $\Omega = [-1, 0] \times [-1, 1] + [0, \cos\phi_2] \times [x \sin\phi_2 - 1, x \sin\phi_2 + 1]$ with velocity field $(v_1, v_2) = (10, 10)$ and negligible diffusion $D = 10^{-7}$ on two grids, one of which is rotated slightly with respect to the other, $\phi_1 = \psi = 0$, $\phi_2 = \arctan(0.5)$. To study the effect of interface coupling on the spatial discretization error, we take a small time step $\Delta t = 10^{-4}$. A cone $c(x, y) = 10^{-8\left((x+\frac{1}{2})^2+(y+\frac{1}{2})^2\right)}$ is taken as initial condition.

The error in the numerical solution consists of both space and time discretization errors made in the interior of the subdomains, and coupling errors made at the interface. The error introduced at the interface can be visualized by following the peak of the initial condition while it propagates from the first to the second subdomain and

plotting the error in the numerical solution at the exact spot of the peak. Bilinear interpolation is used when this spot does not coincide with a grid point, resulting in an interpolated value $c^*(t)$ (which explains the 'hops' in the figures). Although this adds interpolation errors to these figures, tendencies for the development of the discretization error can still clearly be noticed in the figures. Figure 3 shows the error

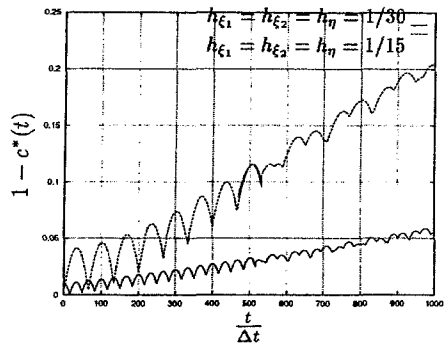

Figure 3 Error development at peak spot, $\Delta t = 10^{-4}$.

development at the peak for this Example 1, for two different mesh sizes. We clearly observe that at the interface virtually no error is introduced, since no jump takes place at $\frac{t}{\Delta t} = 500$. We also recognize the second-order accuracy of the scheme in space. Note that the error in both subdomains grow equally fast, although the space discretization error is expected to be smaller in subdomain 2 where the grid has been rotated in the direction of the flow.

In addition we verify the transparency of the coupling by comparing the accuracy of the discrete solution when increasing the number of interfaces for a problem of fixed size. The advection problem of Example 1 is solved on a decomposition of 20 thin strips, each strip covered by a grid of 5×62 points, which includes a row of virtual points at all sides. We set $\phi_{2k+1} = 0$ for the odd-numbered subdomains and $\phi_{2k} = \arctan(0.5)$ for the even-numbered subdomains. This gives rise to a 'stairway' pattern of subdomains, the solution on which (Figure 4) should be comparable to the previously computed numerical solution for $h = \frac{1}{30}$ since the number of grid points at which the PDE is discretized in the interior of subdomains is the same. The accuracy of the solution on 2 and 20 strips turned out to be indeed comparable; the difference in the error development at the peak spot was less than 5 %.

6 Concluding remarks.

We have presented a patched-grid domain decomposition method in which subgrids may vary per subdomain. The patching of the solution at subdomain interfaces is provided for by optimized interface conditions. Such optimized interface conditions have been designed to meet accuracy requirements as well as convergence rate requirements. The method is discussed here for non-overlapping strip decompositions

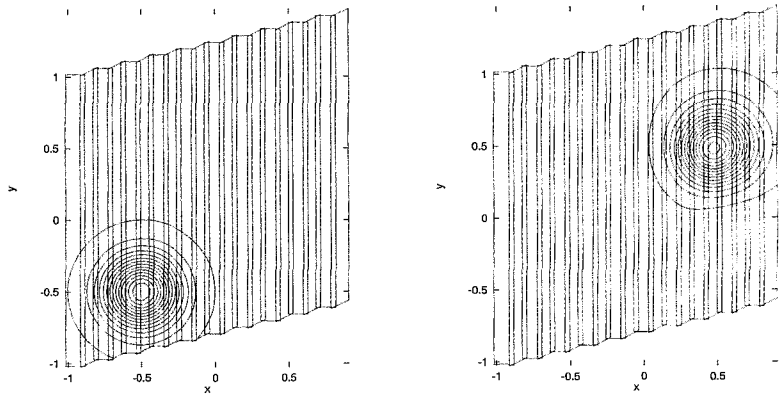

(a) initial condition at t=0 b) computed solution at t=0.1

Figure 4 Multiple interfaces.

and simple structured grids only, but can be extended to any decomposition into non-overlapping subdomains and any grid transformation, due to the formulation of the coupling conditions in terms of local normal and tangential derivatives at the interfaces, which are then transformed to the local computational coordinate system.

REFERENCES

[EES83] Eisenstat S. C., Elman H. C., and Schultz M. H. (April 1983) Variational iterative methods for nonsymmetric systems of linear equations. *SIAM J. Numer. Anal.* 20(No. 2): 345–357.

[QL88] Quarteroni A. and Landriani G. S. (June 1988) Iteration by subdomains in numerical fluid dynamics. 3rd German-Italian Symposium on Applications of Mathematics in Technology.

[SF93] Sleijpen G. L. G. and Fokkema D. R. (1993) BiCGstab(ℓ) for linear equations involving unsymmetric matrices with complex spectrum. *ETNA* 1: 11–32.

[Tan92] Tang W. P. (March 1992) Generalized Schwarz splittings. *SIAM J. Sci. Stat. Comput.* 13(2): 573–595.

[Tan95] Tan K. H. (May 1995) *Local Coupling in Domain Decomposition.* PhD thesis, University Utrecht, faculty Mathematics and Informatics.

[TB93] Tan K. H. and Borsboom M. J. A. (1993) On generalized Schwarz coupling applied to advection-dominated problems. In Keyes D. E. and Xu J. C. (eds) *Domain Decompositions Methods for Partial Differential Equations, Proc. 7th. Int. Symp. on*, pages 125–130. AMS.